Scattering and attenuation properties of Emiliania huxleyi cells and their detached coccoliths

Kenneth J. Voss

Department of Physics, University of Miami, Coral Gables, Fl. 33124

William M. Balch

Bigelow Laboratory for Ocean Sciences, McKown Point, West Boothbay Harbor, Me. 04575

Katherine A. Kilpatrick

Division of Meteorology and Physical Oceanography, Rosenstiel School for Marine and Atmospheric Science, University of Miami, 4600 Rickenbacker Causeway, Miami, Fl. 33149.

Abstract

Measurements of the spectral scattering and attenuation properties of coccolithophores (E. huxleyi; clone 88E) and their associated coccoliths were made for three growth phases as well as for acidified cultures. These measurements allow a clean separation and determination of the optical effects of the various components. The specific beam attenuation coefficients, $m^2(particle)^{-1}$, were found to be 5.17E-12, 7.43E-10, and 7.88E-11 for coccoliths, plated cells and naked cells respectively at 440 nm. The spectral dependence of these factors followed a power law dependence, with a wavelength exponent of -3.7, -0.28, and -0.38 for the coccoliths, plated cells and naked cells respectively. The volume scattering functions for all appeared similar, however the specific backscattering coefficients ($m^2(particle)^{-1}$) at 456 nm were 1.37E-13, 6.72E-12, and 9.90E-13 for coccoliths, plated cells, and naked cells, respectively. The wavelength dependence of this parameter also followed a power law and was -1.4 , -1.2 and -1.0 for the coccoliths, plated cells and naked cells. Overall these results show that optical properties of

a coccolithophore bloom are sensitive to the coccolith/cell ratio and can vary between and within blooms.

Introduction

The coccolithophore Emiliania huxleyi (Lohm.) Hay and Moler, strain 88E, is a ubiquitous species in the worlds oceans, common in both bloom and nonbloom conditions (Green and Leadbeater, 1994). It has a major effect on carbon flux in the oceanic system and, through effects on the optical properties of the water column, on remote sensing. E. huxleyi produces calcite coccoliths which cover the cell, increasing its effective index of refraction changing it's scattering properties. It can also release these coccoliths, adding free coccoliths to the water column and, growing more, continue to release these, until the optical effects of free coccoliths in the water column become significant. Finally, as with other phytoplankton, the cells themselves, quite apart from coccoliths, will add to the water column attenuation and scattering. To determine the relative optical effect of free coccoliths and plated or naked cells, these optical properties must be determined separately in some manner. In field experiments, optical effects of calcite coccoliths have been isolated by bubbling with CO_2 or adding acid (Kilpatrick et al, 1994). However in this process both coccoliths attached to cells and detached in the medium are dissolved, thus separating components is difficult. Laboratory cultures of E. huxleyi can be grown which allow easier manipulation, cleaner interpretation, and separation of the optical signatures of the various components of this species. The measurements reported in this paper are the first separate determinations of the optical properties of spectral backscattering, b_b, and spectral beam attenuation, c, for coccoliths, plated cells, and naked cells.

Methods

Experimental Design - In this experiment, volume scattering and attenuation were measured for cultures of E. huxleyi in three distinct growth phases. We also measured these optical parameters in acidified samples of the same cultures, which allowed resolution of the scattering and attenuation properties of pure suspensions of naked (unplated) cells.

In the first growth phase, cells were in stationary growth (henceforth referred to as "stationary phase" cells). In this phase the cells were predominately (95%) naked and in the sample along with free coccoliths. When this sample is acidified the free coccoliths from the sample are dissolved. Many studies have been performed which have shown that optical properties such as b_b of the cells are not changed during the acidification process (Balch et al, 1992, 1996a, 1996b: Balch and Kilpatrick, 1996). As such, measurement of attenuation or scattering before and after acidification allowed the distinct determination of the optical signature of unplated cells combined with free coccoliths, unplated cells separately, and by difference, free coccoliths.

In the second experiment, a culture was used which was in log phase growth (henceforth referred to as "log"). In this case, most of the cells were plated (80%) and there were also free coccoliths. Optical measurement of the total sample then yielded a combination of plated cells, free coccoliths, and a few naked cells. The acidified sample allowed measurement of the optical properties of unplated cells. Hence, the optical properties of particle types could be resolved with these two samples in their two phases (log and stationary, acidified and non-acidified).

A third independent sample, an older culture (where 50% of the cells had lost their coccoliths) was measured (referred to as "senescent"). In this case only scattering measurements were performed. In this sample the values derived from the other two growth phases were combined with cell and coccolith count information to find an estimate of the relevant optical properties, and these modeled values compared with the values obtained by direct measurement.

More details on the measurement procedures follows.

Cultures - Three cultures of E. huxleyi (clone 88e) were grown in 10 liters of K media (Keller et al. 1987). Cultures were grown in an incubator at 19° C and a 12:12 light:dark cycle at a PAR (photosynthetically available radiation) illumination of 51 $\mu E\ m^{-2}\ s^{-1}$. Cell

and coccolith counts were made daily to follow the growth of the culture and extent of platedness. Aliquots of the culture were removed for optical measurements when the cells were in log, stationary, and senescent growth phases. Cell sizes (diameters) were previously measured to be: 6.4 μm for cells with coccoliths, 5.2 μm for cells without coccoliths. The free coccoliths were approximately 3 μm in length and 2.4 μm in width, the surface area was 13 μm^2 (Fritz, 1997). All measurements were performed at the same time each day to avoid possible problems with diel variability.

Microscope counts - Cells and free coccoliths were counted in a Palmer Maloney chamber using an Olympus BH-2 epi-fluorescence microscope with polarization optics. Cells were examined under both polarization and epi-fluorescence to determine the ratio of plated and naked cells in culture. The free coccoliths in solution were counted under polarization only. Microscopic particle counts were made daily on the original cultures and during the optical experiments after each addition of culture to the experimental tank.

Tank preparation - A blackened 210 liter drum was filled with fresh seawater taken from Bear Cut, off the RSMAS, Univ. of Miami dock and filtered overnight by recirculating the water through a 0.2 μm poresize Gelman pleated filter cartridge attached to a Mini-Giant submersible pump. The filter cartridge was removed before each experiment and the Mini-Giant remained in the drum to re-circulate the seawater during measurements. The temperature in the drum was maintained at 19 °C by a cooling coil made from tygon tubing which was attached to a re-circulating water bath chiller.

Optical measurements - Spectral attenuation of the stationary and log phase cultures were made with the Vislab Spectral Transmissometer (VLST). (Petzold and Austin 1968) These measurements were done at 5 wavelengths: 440 nm, 490 nm, 520 nm, 550 nm, and 670 nm. Light scattering measurements were done with the General Angle Scattering Meter (GASM) (Petzold 1972) at 6 wavelengths: 440, 490, 520, 550, 610, and 670 nm.

The volume scattering function (*VSF*) was measured with this instrument at every degree between 10 and 170 degrees from the incident beam. Light scattering was also measured using a Brice Phoenix (BP) scattering photometer at three angles, 45, 90 and 135 degrees, and at two wavelengths, 436 nm and 546 nm. The VLST and GASM are designed to be in-situ devices, hence they require a large enough sample to immerse the instrument. This immersion was done by placing the instruments in the tank of 0.2 μm filtered seawater and sequentially adding culture aliquots. The BP measures a much smaller sample (beam size = 4 x 15 mm) which allowed much more sample manipulation (e.g. acidification).

The procedure followed for each instrument was as follows. GASM and VLST were placed in the tank filled with filtered seawater. The spectral attenuation, *c*, and *VSF*, of the background seawater were measured, and a sample removed for the BP measurement. The BP measured the *VSF* for this sample, and the sample was acidified by adding 6.4 ml of 1.2% glacial acetic acid per liter seawater to the cuvette and the *VSF* measured again. There was no significant difference between the measured *VSF* for the acidified and non-acidified cases in this background seawater sample. At this point an aliquot of the culture sample was added to the water, and the barrel was stirred with an electric pump until the transmissometer readings stabilized. A subsample of this container was removed for measurement by the BP and particle counts, then GASM and VLST measurements were performed. Following the BP measurement the aliquot was acidified and the *VSF* remeasured. E. huxleyi culture was added to the tank to achieve three concentrations and measurements performed at each stage. The maximum optical pathlength (c* geometric pathlength) measured was approximately 0.2, thus multiple scattering effects were not significant. After the last culture addition the entire tank was acidified to dissolve all calcite coccoliths by adding 6.4 ml of 1.2% glacial acetic acid per liter seawater bringing the pH to 5.5, whereupon measurements were performed both in the drum and with the BP. At this point the BP sample was acidified again to confirm that the coccoliths had been totally dissolved in the first case. This procedure was followed for each of the three cultures,

however for the senescent case the VLST was malfunctioning so no spectral attenuation measurements were available.

The VLST directly measures the spectral transmission over a 1 meter path, $T(\lambda)$, which is converted to the spectral beam attenuation, $c(\lambda)$, by the equation:

$$c(\lambda) = -\ln(T(\lambda)) \ .$$

No correction was made for the finite (about 1.5 degree) acceptance angle of the transmissometer. This effect is estimated to cause a 10% underestimate of c (Voss and Austin, 1993).

The backscattering coefficient, b_b, was calculated with the measurements of the VSF in two ways. Since the GASM measurements only extend to 170 degrees, the data was extrapolated to 180 degrees by assuming $VSF(\theta)$ for 170 to 180 degrees is constant. The data was then integrated directly to obtain b_b through the equation:

$$b_b = 2\pi \int_{90^\circ}^{180^\circ} VSF(\theta)\sin(\theta)d\theta$$

While more sophisticated extrapolation methods might be hypothesized, because the solid angle between 170° and 180° is such a small part of the total hemisphere and $VSF(\theta)$ is approximately flat in this region, the portion of b_b form 170 to 180 degrees only contains 1% of the total b_b. Thus this is probably only a +-1% error in the calculation of b_b.

For the BP, data was only obtained at three angles (45, 90, and 135). To interpolate and extrapolate these measurements to obtain the VSF from 90-180 degrees, these data were used to fit the equation (Beardsley and Zaneveld, 1969; Gordon, 1976):

$$VSF(\theta) = \frac{f}{(1 - g\cos(\theta))^4 (1 + h\cos(\theta))^4}.$$

Once the coefficients for this equation (f, g, and h) were determined, the equation was numerically integrated to obtain b_b. A test of this method was performed in which the GASM data was directly integrated to obtain b_b and the values of the VSF at the three angles used to derive a b_b through the analytical fit. This was done for all the GASM measurements and the results can be seen in Figure 1. As can be seen this technique works well (the standard deviation was 6%), indicating that the b_b derived from the fitted analytic equation is accurate.

Results

Spectral beam attenuation - As previously introduced, we made two types of measurements for beam attenuation, the stationary cell case and the log case which provided three independent variables, concentrations of 1) naked cells, 2) plated cells, and 3) free coccoliths. The dependent variable is the measured beam attenuation. We also examined three concentrations of each growth phase (stationary and log), and the acidified sample. In total, for the beam attenuation, we have 8 measurements of beam attenuation, with associated cell and coccolith counts. A linear, multivariable, least squares analysis (Natrella, 1963) was performed, fitting the experimentally measured beam attenuation data to the equation:

$$c(\lambda) = x(\lambda)\ X + y(\lambda)\ Y + z(\lambda)\ Z,$$

where X was the concentration of naked cells (cell m^{-3}), Y was the concentration of plated cells (cell m^{-3}), and Z was the concentration of coccoliths (coccolith m^{-3}). The parameters determined in the fit were $x(\lambda)$, $y(\lambda)$, and z (λ), the beam attenuation per naked cell, plated cell, and coccolith concentrations, respectively. In this way the relative contribution to the beam attenuation for each component could be determined. The resulting specific beam attenuation coefficients, and their standard deviations, for the different wavelengths are shown in Table 1 and in Figure 2. The error for the free coccoliths is fairly large, mainly because we had few samples (relative to the b_b measurements) to work with. These still are

informative as they give a qualitative view of the relative magnitude of these coefficients. A typical result of how well the above equation fits the data is shown in Figure 3. This is the experimentally measured c(440 nm) vs the modeled c values, using the empirically determined coefficients from the above equation. The average absolute error in the predicted c values was 25%. In all cases the worst prediction was for the acidified sample for the log case, when this point is excluded the average absolute error is less than 20%. The cell coefficients can be compared to the measurements of Bricaud and Morel (1986). By using their Table III the specific beam attenuation coefficient of E. huxleyi can be derived as 1.94E-10 (cells m^2) (435 nm) and 1.72E-10 (cells m^2) (550 nm). There is no information in this paper as to the state of the coccolithophores, however these values fall between our values for naked and plated cells.

The first important point to note in this data is the wavelength dependence of the factors. Each of these factors can be fit to a power law wavelength dependence (λ^{α}). The plated cell and naked cell factors are spectrally flat, with wavelength exponents of -0.3 and -0.4 respectively. This agrees well with the value derived from the Bricaud and Morel (1986) measurements (-0.5). The coccolith specific beam attenuation coefficients are strongly wavelength dependent (a wavelength exponent of -3.7), but this is strongly influenced by the 670 nm data point. Without this point the wavelength exponent is -2.4, still strong but significantly less than -3.7. Secondly it is important to note the relative magnitude of the factors, increasing by roughly an order of magnitude between the coccolith, naked cell and plated cell. The specific beam attenuation coefficient for the plated cells were more than 100 times greater than free coccoliths, this factor was greater than the number of coccoliths plating each cell (~ 30; Fig. 3).

Spectal light scattering - The normalized *VSF* for all of the samples showed no significant spectral dependence (as reported for field measurements during E. huxleyi blooms, Balch et al 1991). The normalized *VSF* at each wavelength is shown in Figure 4. As can be seen there was also no marked difference in the normalized *VSF* between the

various samples. Because we have no measure of the *VSF* between 0 and 10 degrees it is not possible to comment on the total scattering coefficient, b. However b_b, the backscattering coefficient is perhaps a more important parameter because of it's impact on remote sensing reflectance and diffuse attenuation.

As mentioned above we can derive b_b from both the GASM and BP measurements. The b_b measured for each sample, for the blue (440 nm for GASM, 436 for BP), and green (550 nm for GASM and 546 for BP) are shown in Figure 5. As can be seen from these figures, for the most part, the measurements with BP and with GASM agree well, but there are some deviations. Each instrument has specific advantages. GASM allows measurement of much more of the *VSF* (10-170 degrees) and more wavelengths (6), but BP allows more manipulation of the sample. This is primarily because GASM requires immersion, thus we did not logistically have enough culture to repeatedly bring the 210 liter tank to a given cell and coccolith concentration, acidify and then start again. The BP allowed us to acidify each sample, thus gaining more information in each case.

As with the spectral c case, we performed a multiple linear fit to b_b which isolated the specific b_b coefficients (b_b*) for coccolith, plated cells and naked cells. Because b_b is an additive property, the linear, multivariable, least squares fit took the following form:

$$b_b(\lambda) = x(\lambda)X + y(\lambda)\ Y + z(\lambda)\ Z,$$

where once again X, Y, and Z were the coccolith, plated cell, and naked cell concentrations. Hence $x(\lambda)$, $y(\lambda)$ and $z(\lambda)$ represented the b_b* for coccoliths, plated cells, and naked cells. Table 2 shows the BP derived coefficients and the GASM derived coefficients. Figure 6 shows the same data graphically. Note the 520 nm measurement with GASM was probably an overestimate as it was anomalously high in all the measurements with this instrument (but no reason has been found for this problem, so the measurements are reported "as is"). First we note that the GASM coefficients are somewhat larger than the BP coefficients (but within the standard error), particularly in the

blue. The BP derived coefficients have lower standard error than the GASM derived coefficients. This is because the acidified measurements could be performed on every sample, versus the end points for GASM, as discussed above. The previous work by Bricaud and Morel (1986) have no experimental measurements of b_b for E. huxleyi, however they do show theoretical Mie scattering calculations for this parameter. These calculations predict a positive exponent for the wavelength dependence of b_b, however the wavelength dependence determined form the GASM measurements leads to a power law dependence on wavelength with an exponent of -1.4, -1.2, and -1.0 for the coccolith, plated cell and naked cell component respectively. Naked cells should be similar to typical phytoplankton cells, which have a relatively low average relative index of refraction (1.05 or less, relative to water (Mobley, 1994)). A wavelength dependence -1 is what is commonly assumed for the wavelength dependence of the total scattering coefficient (Gordon and Morel, 1983). Plated cells will have a higher relative index of refraction because of the calcite coccoliths, and in this case show a larger wavelength dependence. Free coccoliths, with their high relative index of refraction and small size have the largest wavelength dependence, which could cause a signature in remotely sensed images if differences in the visible bands are viewed.

While in field cases it is not possible to get a separate number for the b_b* of plated cells and naked cells, some estimates of the b_b* due to coccoliths have been made. The $b_b{*}_{coccolith}$ from the BP measurements (1.37E-13 and 1.27E-13 m^2 $coccolith^{-1}$) are close to the field measurements reported in Balch et al.(1991) of 1.41E-13 and 1.29E-13 m^2 $coccolith^{-1}$ for the 436 and 546 nm respectively. Field measurements of $b_b{*}_{coccolith}$ should be an overestimate due to neglecting the contribution of plated cells, but this does not appear to have been the case in this situation. Note that in the Balch et al. data set, the ratio of free coccoliths to cells reached values of 400 or more, thus the free coccoliths dominated the optical properties, the contribution by plated cells was negligible (as will be discussed below).

Besides the wavelength dependence of these factors it is useful to look at the absolute magnitude of the b_b*. As can be seen, it varies between components by less than the beam attenuation coefficients. This is because small particles (in this case coccoliths) tend to direct more of the scattered light in the backward direction causing them to be more efficient backscatterers. Thus the ratio of $b_b{}^*_{\text{coccolith}}$ to the $b_b{}^*_{\text{plated cell}}$ is on the order of 40 rather than 100 as in the case of c.

If these b_b* coefficients are relevant for field samples we can use them to look at the relative importance of free coccoliths to plated cells in determining the optical signature of the ocean for bloom conditions. To test these coefficients a data set obtained during a coccolithophore bloom off of Iceland (Holligan et. al. 1993; Balch et. al. 1996a and b) was used. This data set had counts of live cells and free coccoliths along with b_b measurements. Figure 7 illustrates the fit to the measurements, using the specific bb coefficients derived above and the cell count data form the cruise, for the blue and green wavelengths of BP. The value shown in Figure 7, bb', is the acid labile b_b, which is b_b total minus b_b acidified and is effectively the b_b for the calcite in the sample. The coefficients used in the model were from the ones derived from the BP measurements of the laboratory cultures. The 1:1 line is shown along with a line representing the best fit. There seems to be an overestimate of the field data by 20%, but overall the model seems to do a reasonable job of estimating the field data. The importance of this work is in showing the relative importance of the components in determining the optical properties. With counts of the separate components, we can determine the relative contribution of the plated cells and coccoliths to the total b_b in this situation. Figure 8 illustrates the portion of b_b due to plated cells versus b_b'. b_b' should include contributions from plated cells and free liths. It appears that in this data set b_b' is dominated by plated cells. If one looks at the ratio of free coccoliths to plated cells, it is obvious that in this study the high b_b' cases are those dominated by cells (i.e. low detached coccolith to plated cell ratio). Since the ratio of free coccoliths/cells can vary from bloom to bloom, the importance of free coccoliths versus

cells in determining the optical properties can vary. For example, Balch et al. (1991) reported coccolith/cell ratios for blooms occurring in the Gulf of Maine for two years, 1988 and 1989. In the first case the highest free coccolith/cell reported were about 50, indicating that coccoliths would have had approximately equal importance as cells in determining the backscattering. In the 1989 bloom, the coccolith/cell ratio reached values over 400, and in this case the free coccoliths would have been the dominate constituent. The coccolith/cell ratio can vary within blooms and non-bloom waters which makes this an important ratio to understand in interpretation of remote sensing reflectance.

Conclusions

We have found the specific backscattering and spectral beam attenuation coefficients for the separate components of coccoliths, plated cells, and naked cells. These show that the plated cell contribution to the optical properties can be greater than the sum of the coccoliths coating them. Thus the optical properties of a coccolithophore bloom are sensitive to the ratio of free coccoliths to plated cells. Since the spectral variation of b_b^* is different for these coefficients, the remote sensing reflectance will vary with this ratio, with the stronger spectral variation when free liths dominate the upper water column. This ma be the reason that blooms with a high ratio free liths are most evident in satellite images based on color differences techniques.

Acknowledgments

This work was supported by the Ocean Optics program of the Office of Naval Research under contracts #N00014-95-10309 (KV). WMP was supported by the ONR Ocean Optics program (N00014-91-J-1048), NASA (NAS5-31363 and NAGW 2426) and NSF(OCE90-22227 and OCE-9596167). We would also like to thank Al Chapin for his help in making these measurements.

References

Balch, W. M., P. M. Holligan, S. G. Ackleson, and K. J. Voss. 1991. Biological and optical properties of mesoscale coccolithophore blooms in the Gulf of Maine. Limnol. Oceanogr. **36**: 629 - 643.

Balch, W. M., P. M. Holligan and K. A. Kilpatick. 1992. Calcification, photosynthesis and growth of the bloom-forming coccolithophore, Emiliania huxleyi. Cont. Shelf Res. 12: 1353-1374.

_____ and K. A. Kilpatrick. 1996. Calcification rates in the equatorial Pacific along 140W. Deep Sea Research. 43:971-993.

_____, _____, P. M. Holligan, and C. Trees. 1996a. The 1991 coccolithophore bloom in the central north Atlantic I - Optical properties and factors affecting their distribution. Limnology and Oceanography. 41: 1669-1683.

_____, _____, _____, D. Harbour, and E. Fernandez. 1996b. The 1991 coccolithophore bloom in the central north Atlantic II - Relating optics to coccolith concentration. Limnology and Oceanography. 41: 1684-1696.

Beardsley, G. F. and J. R. V. Zaneveld. 1969. Theoretical dependence of the near-asymptotic apparent optical properties on the inherent optical properties of sea water. J. Opt. Soc. Am.. **59**: 373-377.

Fritz, J. J. 1997. Growth dependence of coccolith detachment, carbon fixation, and other associated processes by the coccolithophore Emiliania huxleyi. Univ. Miami. Ph.D. Thesis, Rosenstiel School for Marine and Atmospheric Sciences, Miami, Fl. 179 pp.

Gordon, H. R.. Radiative transfer in the ocean: A method of determination of absorption and scattering properties. Appl. Opt. **15**: 2611 - 2613.

Gordon, H. R. and A. Morel. 1983. Remote Assessment of Ocean Color for Interpretation of Satellite Visible Imagery, a Review; Lecture Notes on Coastal and Estuarine Studies, Volume 4. Springer Verlag.

Green, J. C. and B. S. C. Leadbeater. 1994. The Haptophyte Algae. Oxford Science Publications, The Systematics Association Special Volume No 51. Clarendon Press: Oxford. 446 pp.

Holligan, P. M., E. Fernandez, J. Aiken, W. M. Balch, P. Boyd and others. 1993. A geochemical study of the coccolithophore Emiliania huxleyi. In the North Atlantic Global Biogeochemical Cycles. **7**: 879-900.

Keller, M. D., R. C. Selvin, W. Claus, and R. R. L. Guillard. 1987. Media for the culture of oceanic ultraphytoplankton. J. Phycol.. **23**: 633-638.

Kilpatrick, K. A., Y. Ge, W. M. Balch, and K. J. Voss. 1994. A photometer for the continuous measurement of Calcite-dependent light scatter in seawater. Proc. Soc. Photo-Optical Instrumentation, 1994: 512 - 521.

Mobley, C. D.. 1994. Light and Water, Radiative Transfer in Natural Waters. Academic Press.

Natrella, M. G. 1963. Experimental Statistics. National Bureau of Standards Handbook 91. U. S. Government Printing Office, Washington.

Petzold, T. J.. 1972. Volume scattering functions for selected ocean waters. Univ. Calif. Scripps Inst. Oceanogr. Tech. Rep. 72-78.

Petzold, T. J. and R. W. Austin. 1968. An underwater transmissometer for ocean survey work. Univ. Calif. Scripps Inst. Oceanogr. Tech. Rep. 68-9.

Voss, K. J. and R. W. Austin. 1993. Beam-Attenuation measurement error due to small-angle scattering acceptance. J. Atmospheric and Oceanic Techn.. **10**: 113-121.

Table 1) Specific beam attenuation coefficients. Standard error of the coefficients are shown in parenthesis.

wavelength	$c^*_{coccolith}$	$c^*_{plated\ cell}$	$c^*_{naked\ cell}$
	m^2 (lith)$^{-1}$x10^{12}	m^2 (plated cell)$^{-1}$x10^{10}	m^2 (naked cell)$^{-1}$x10^{11}
440	5.2(3.9)	7.4(3.4)	7.9(3.8)
490	4.1(3.4)	5.9(3.0)	7.3(3.3)
520	3.6(3.3)	5.5(2.9)	7.4(3.3)
550	3.0(3.3)	5.7(3.0)	7.3(3.2)
670	1.1(3.5)	6.3(3.0)	6.6(3.4)

Table 2)

BP derived spectral backscattering coefficients. Standard error of the coefficients are shown in parenthesis.

wavelength	$b_b^*{}_{\text{coccolith}}$	$b_b^*{}_{\text{plated cell}}$	$b_b^*{}_{\text{naked cell}}$
	m^2 (lith)$^{-1}$x10^{13}	m^2 (plated cell)$^{-1}$x10^{12}	m^2 (naked cell)$^{-1}$x10^{13}
456	1.4(0.2)	6.7(1.3)	9.9(2.3)
546	1.3(0.2)	5.8(1.2)	9.5(2.0)

GASM derived spectral backscattering coefficients. Standard error of the coefficients are shown in parenthesis.

wavelength	$b_b^*{}_{\text{coccolith}}$	$b_b^*{}_{\text{plated cell}}$	$b_b^*{}_{\text{naked cell}}$
	m^2 (lith)$^{-1}$x10^{13}	m^2 (plated cell)$^{-1}$x10^{12}	m^2 (naked cell)$^{-1}$x10^{13}
440	2.1(0.2)	8.8(2.4)	1.7(1.7)
490	1.8(0.1)	9.3(1.9)	1.3(1.0)
520	2.2(0.2)	13(2.6)	1.8(1.4)
550	1.6(0.1)	6.6(1.5)	1.1(0.8)
610	1.4(0.1)	5.1(2.3)	1.7(1.2)
670	1.2(0.1)	6.5(1.3)	0.84(0.72)

FIGURE CAPTIONS

Figure 1) Comparison of the b_b derived from the numerical fit to the Beardsly and Zaneveld (1969) equation and b_b found by directly integrating the VSF data.

Figure 2) Specific beam attenuation coefficients as a function of wavelength. Also shown is the power law fit to each component, discussed in the text. The exponent found for each component was -3.7, -0.28 and -0.38 for coccoliths, plated cells, and naked cells respectively.

Figure 3) The measured c is compared with the reconstruction of c using cell counts and the specific attenuation coefficients of the model.

Figure 4) Example VSF(490 nm) for each growth phase (stationary, log and senescent).

Figure 5) Comparison of the BP measurements and GASM measurements of b_b for the same samples.

Figure 6) Specific b_b coefficients (b_b*) as a function of wavelength for both the BP derived and GASM derived measurements. Also shown is the power law fit to each component, discussed in the text. The exponent found for each component was -1.4, -1.2 and -1.0 for coccoliths, plated cells, and naked cells respectively.

Figure 7) Fit of empirical model to data obtained in coccolithophore bloom off of Iceland. b_b' is the acid labile b_b, derived from the b_{btotal} -$b_{bacidified}$ for the field samples. Shown are the 1:1 line and a line showing the best fit between the measured and predicted values.

Figure 8) Relative contribution of the b_b due to plated cells to the acid labile b_b (b_b').

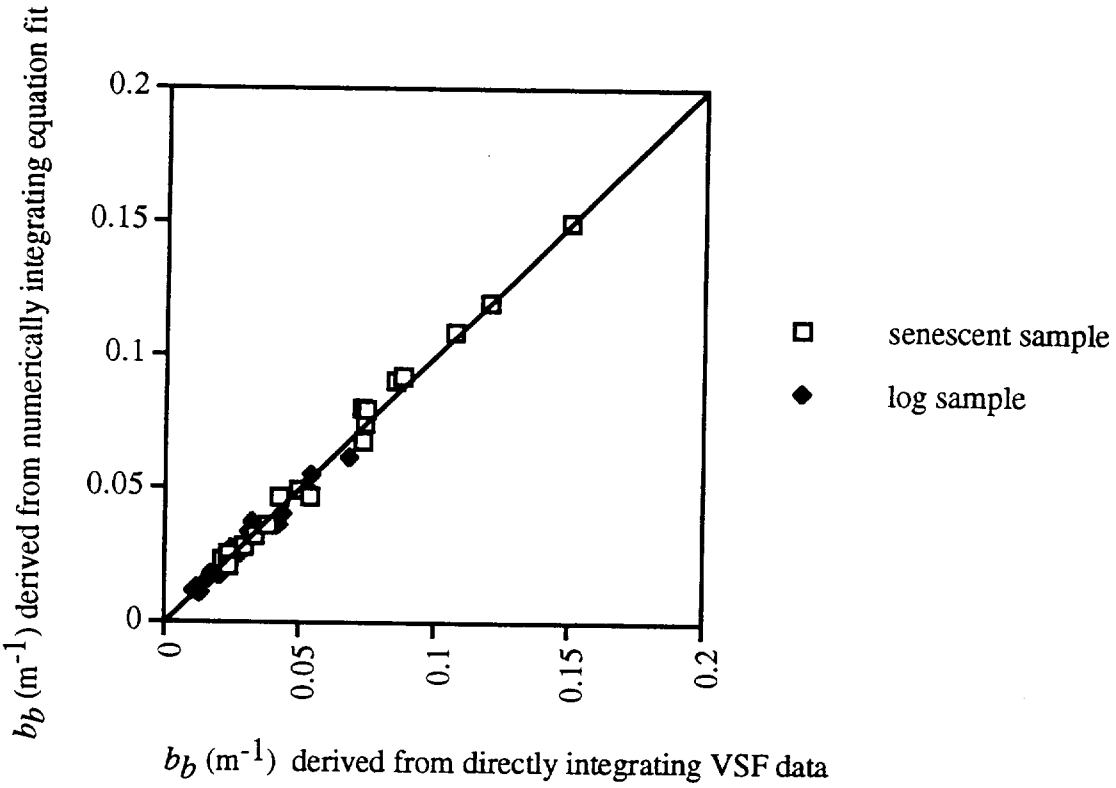
b_b (m^{-1}) derived from numerically integrating equation fit
0.2
0.15
0.1
0.05
0
0
0.05
0.1
0.15
0.2
b_b (m^{-1}) derived from directly integrating VSF data
senescent sample
log sample

FIGURE 1

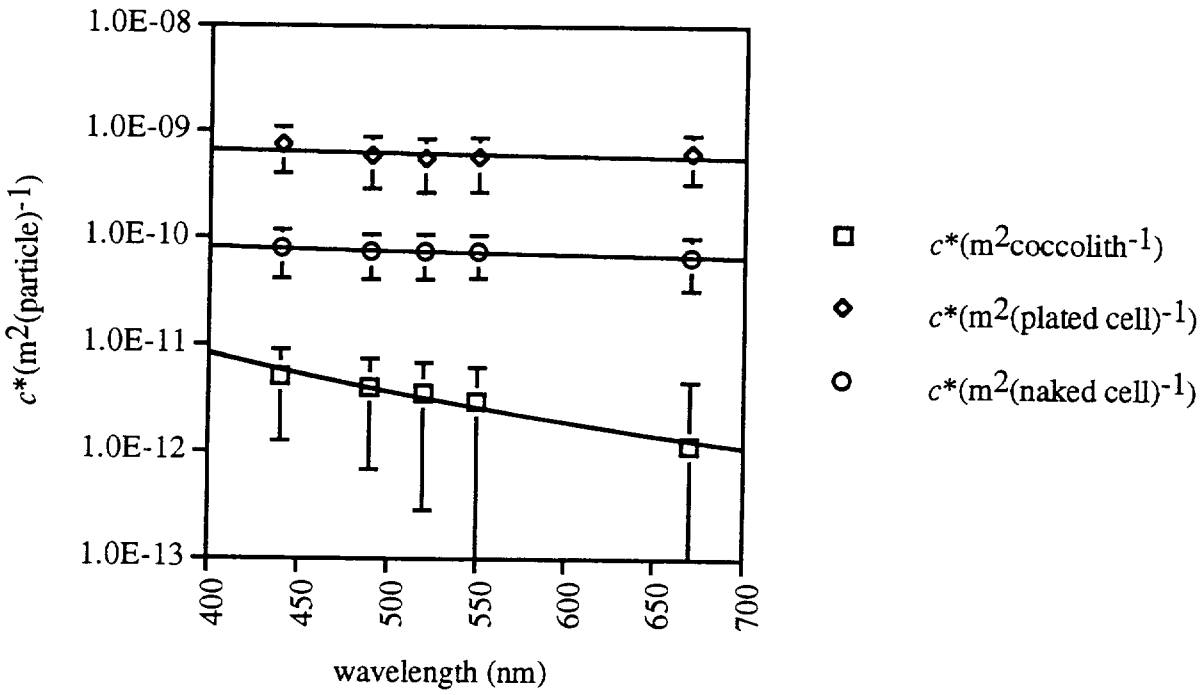
1.0E-08
1.0E-09
1.0E-10
1.0E-11
1.0E-12
1.0E-13
c*(m2(particle)-1)
400
450
500
550
600
650
700
wavelength (nm)
c*(m2coccolith-1)
c*(m2(plated cell)-1)
c*(m2(naked cell)-1)

Figure 2

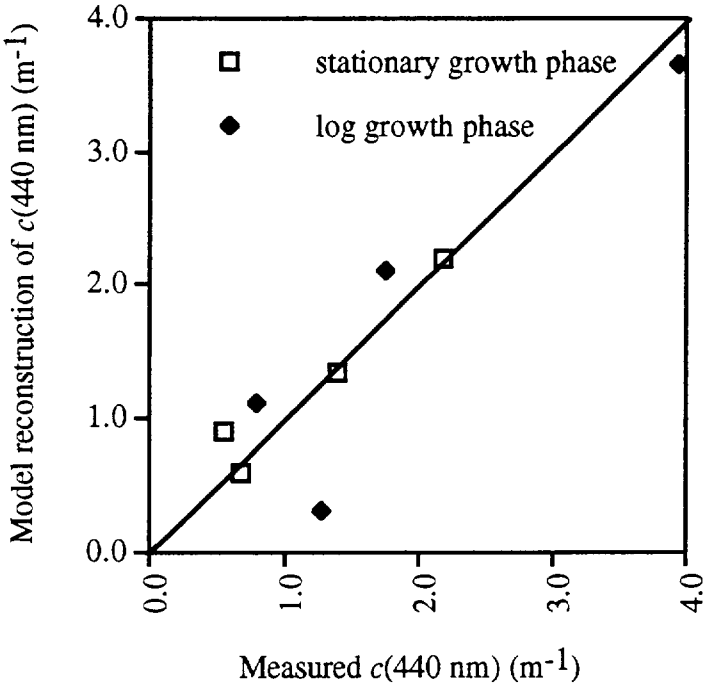
4.0
3.0
2.0
1.0
0.0
Model reconstruction of c(440 nm) (m-1)
stationary growth phase
log growth phase
0.0
1.0
2.0
3.0
4.0
Measured c(440 nm) (m-1)

Figure 3

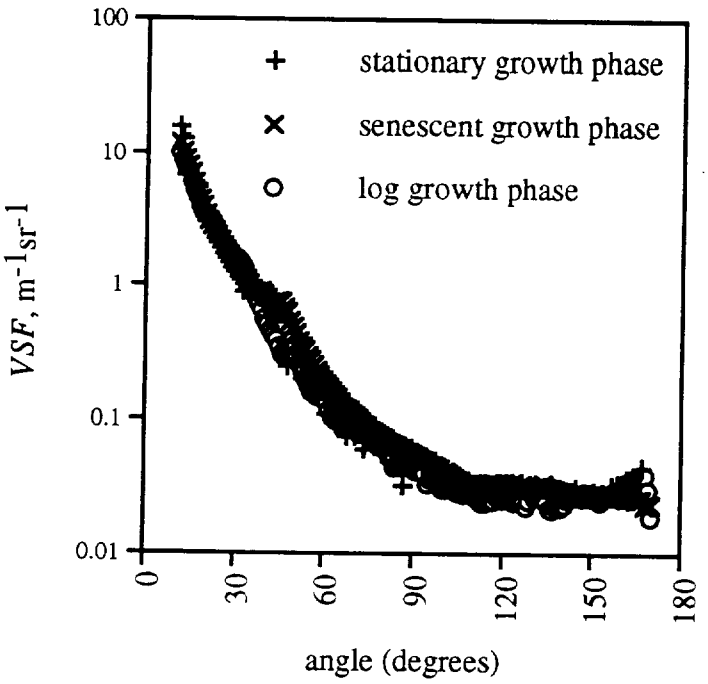
100
10
1
0.1
0.01
VSF, m-1sr-1
stationary growth phase
senescent growth phase
log growth phase
0
30
60
90
120
150
180
angle (degrees)

Figure 4

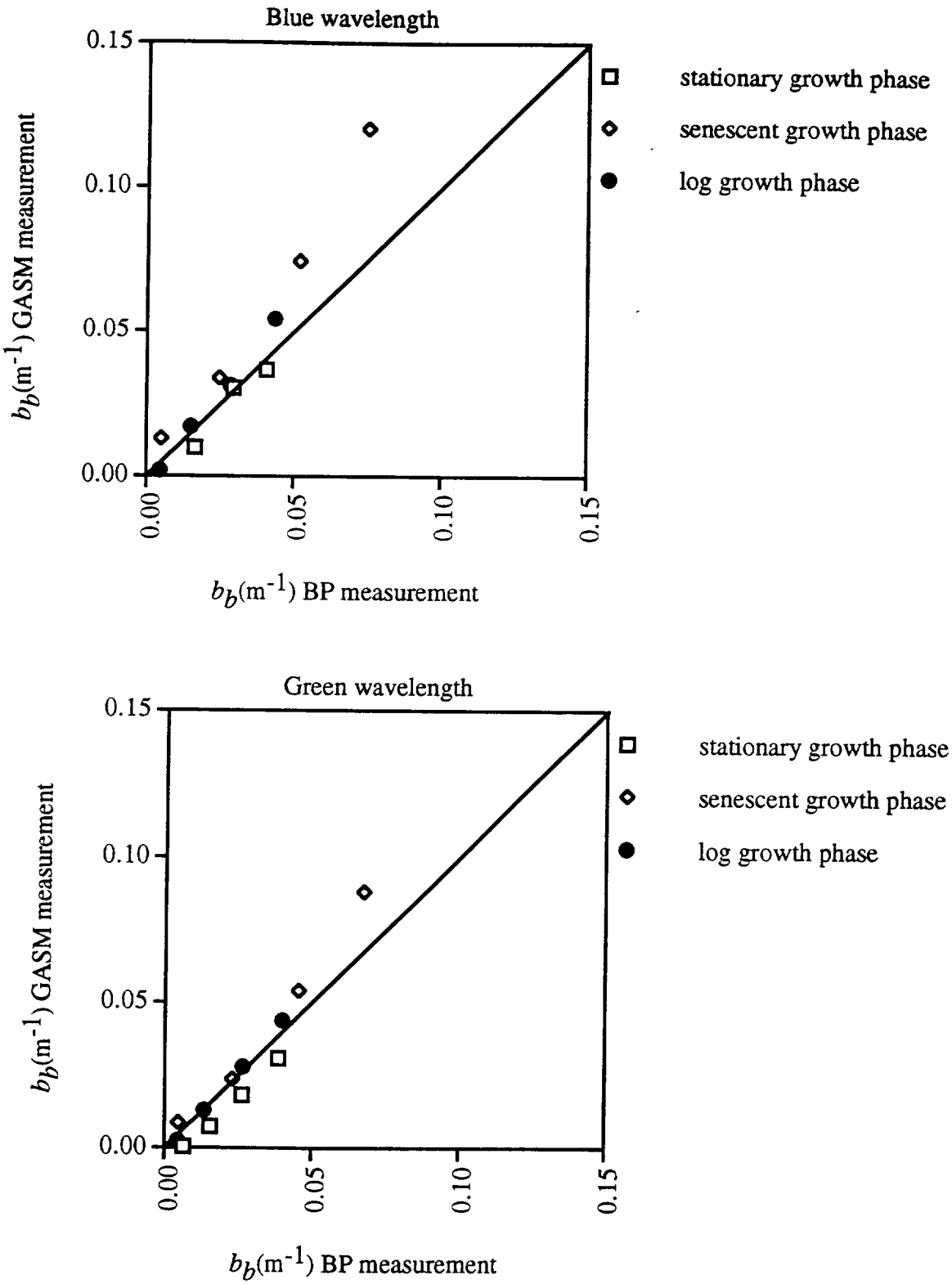
Blue wavelength
0.15
0.10
0.05
0.00
b_b(m^{-1}) GASM measurement
0.00
0.05
0.10
0.15
b_b(m^{-1}) BP measurement
stationary growth phase
senescent growth phase
log growth phase
Green wavelength
0.15
0.10
0.05
0.00
b_b(m^{-1}) GASM measurement
0.00
0.05
0.10
0.15
b_b(m^{-1}) BP measurement
stationary growth phase
senescent growth phase
log growth phase

Figure 5

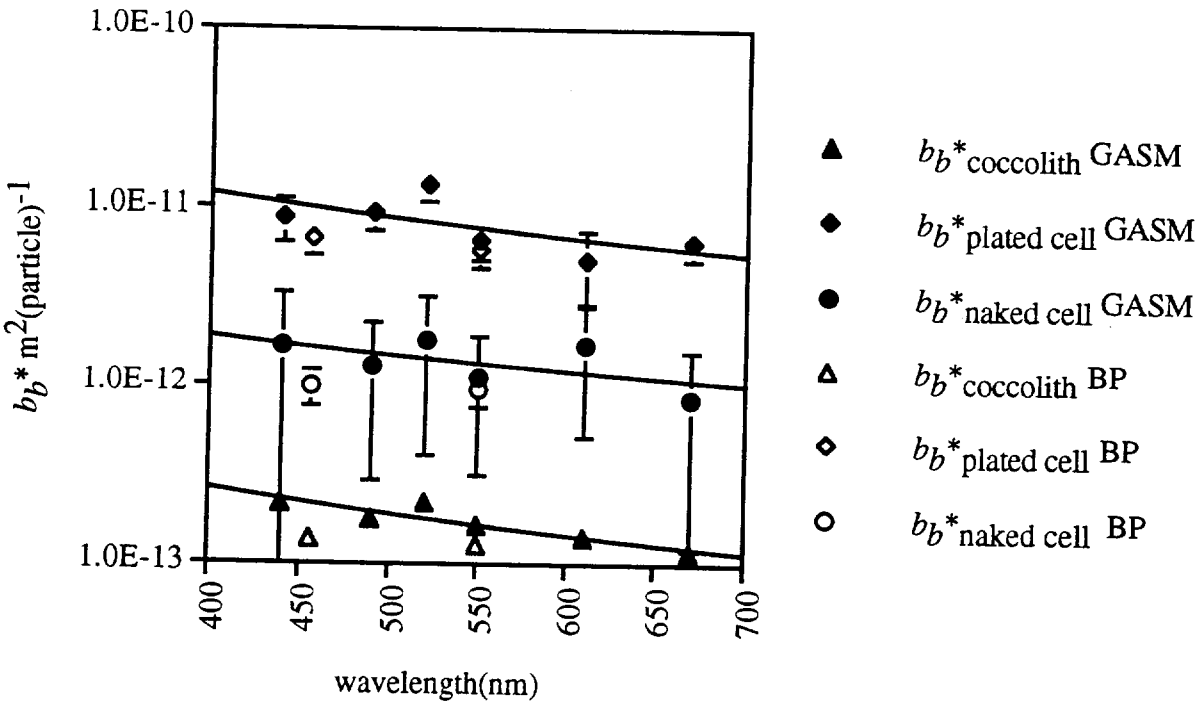
1.0E-10
1.0E-11
1.0E-12
1.0E-13
b_b* m^2(particle)$^{-1}$
400
450
500
550
600
650
700
wavelength(nm)
b_b*coccolith GASM
b_b*plated cell GASM
b_b*naked cell GASM
b_b*coccolith BP
b_b*plated cell BP
b_b*naked cell BP

Figure 6

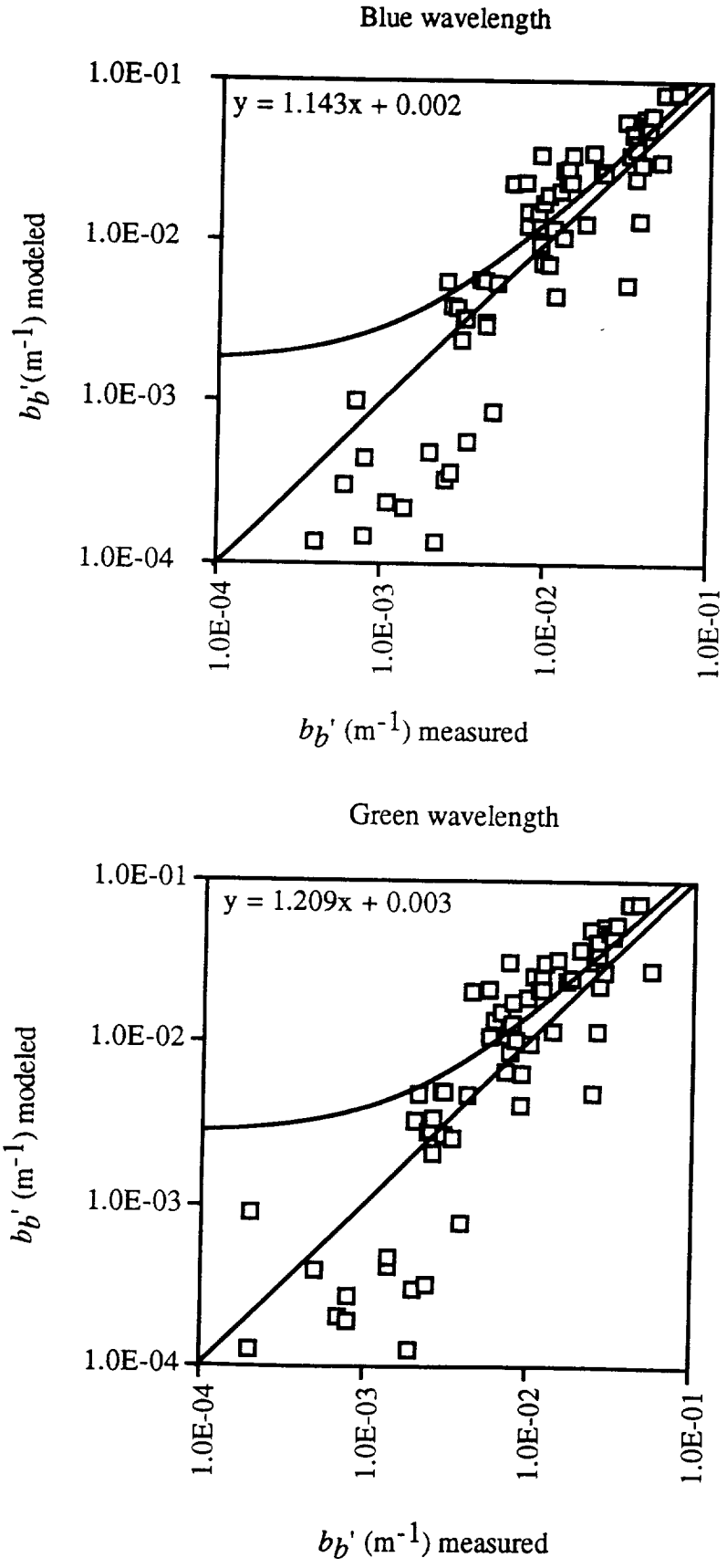
Blue wavelength
y = 1.143x + 0.002
1.0E-01
1.0E-02
1.0E-03
1.0E-04
b_b'(m^{-1}) modeled
1.0E-04
1.0E-03
1.0E-02
1.0E-01
b_b' (m^{-1}) measured
Green wavelength
y = 1.209x + 0.003
1.0E-01
1.0E-02
1.0E-03
1.0E-04
b_b' (m^{-1}) modeled
1.0E-04
1.0E-03
1.0E-02
1.0E-01
b_b' (m^{-1}) measured

Figure 7

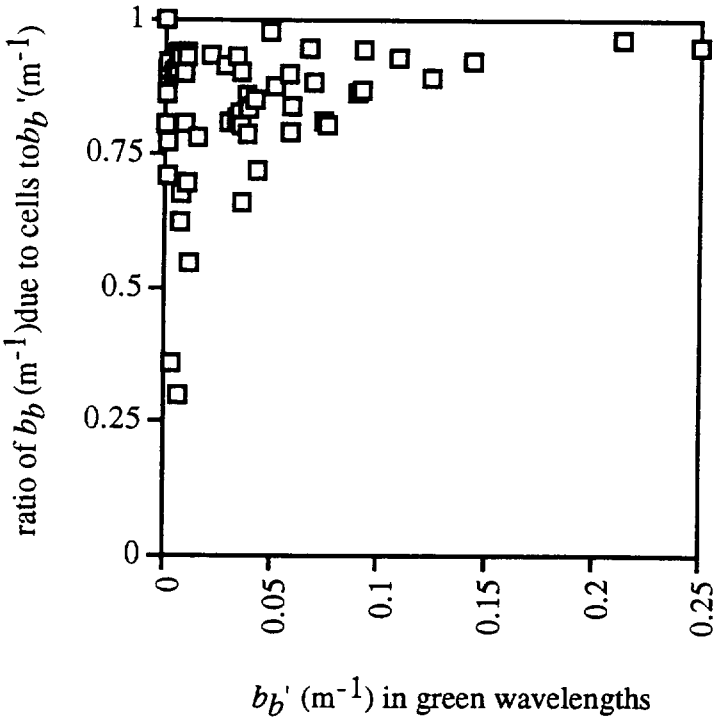
ratio of b_b (m^{-1})due to cells tob_b '(m^{-1})
1
0.75
0.5
0.25
0
0
0.05
0.1
0.15
0.2
0.25
b_b' (m^{-1}) in green wavelengths

Figure 8